

Solubility of Ti in andradite in upper mantle conditions: preliminary results

ANDREA ORLANDO^{1*} and DANIELE BORRINI²

¹ C.N.R.-C.S. Minerogenesi e Geochimica Applicata, Via G. La Pira 4, I-50121 Firenze, Italy

² Dipartimento di Scienze della Terra, Università degli Studi di Firenze, Via G. La Pira 4, I-50121 Firenze, Italy

Submitted, July 2000 - Accepted, February 2001

ABSTRACT. — Piston cylinder experiments were carried out, aimed at determining Ti solubility in andradite in upper mantle conditions (P=1.5-2.0 GPa, T=1200-1300°C). Starting materials were Ti-undersaturated and Ti- saturated (with respect to 1 atm) synthetic andradites. From unreversed experiments at 1.5 and 2.0 GPa, the maximum Ti contents in andradites were determined as 1.0-1.4 atoms per formula unit (a.p.f.u.), compared with 1.5-1.9 a.p.f.u. at 1 atm. Oxygen fugacity was not controlled in experimental runs. The main mechanism controlling the entry of Ti in the garnet structure at high pressure appears to be *schorlomitica* substitution, whereas some *morimotoitic* substitution may occur in Ti- undersaturated andradites.

RIASSUNTO. — In questo lavoro sono riportati i risultati di alcuni esperimenti preliminari effettuati al pistone – cilindro e volti a determinare la solubilità del Ti nelle andraditi in condizioni corrispondenti al mantello superiore (P=1,5-2,0 GPa, T=1200-1300°C). I materiali di partenza sono rappresentati da andraditi sintetiche rispettivamente sottosature e sature in Ti (a 1 atm). A 1,5 e 2,0 GPa il massimo contenuto di Ti nelle andraditi diminuisce rispetto alle condizioni nelle quali la pressione è uguale a 1 atm; gli atomi di Ti per unità di formula diminuiscono infatti da 1,5-1,9 (a 1 atm) a 1,0-1,4 (a

1,5-2,0 GPa). Il ruolo della fugacità di ossigeno nel controllo dell'ingresso del Ti nell'andradite non può comunque essere stabilito dal momento che gli esperimenti al pistone cilindro sono stati eseguiti senza controllare questa variabile. Il principale meccanismo che controlla l'ingresso del Ti nella struttura del granato appare essere la sostituzione *schorlomitica* mentre la sostituzione *morimotoitica* sembra avere una certa importanza solo nell'ambito delle andraditi sottosature in Ti.

KEY WORDS: *Synthetic garnets, titanium andradite, high pressure experiments, piston cylinder.*

INTRODUCTION

Andradite (Ca₃Fe₂Si₃O₁₂) is commonly found in subsilicic alkaline igneous rocks, where it may also occur in its Ti-bearing varieties, melanite (TiO₂ <8 wt%) and schorlomite (TiO₂ >8 wt%; Howie and Woolley, 1968). Ti-andradite is also found in metamorphic rocks which formed in oxidising conditions (e.g., Huckenholz and Yoder, 1971) and as a characteristic phase in hydrothermal alteration assemblages (e.g., Lang *et al.* 1995).

In the potassic Roman magmatic province

* Corresponding author, E-mail: aorlando@geo.unifi.it

(Italy), melanite occurs as phenocrysts and as a groundmass phase in phonolitic trachytic ignimbrites, phonolites and foidites from Monte Vulture volcano (De Fino *et al.*, 1986; Caggianelli *et al.*, 1990; Melluso *et al.*, 1996). The parental magmas of these garnet-bearing rocks probably derived from a mantle source, possibly metasomatised by a subducting slab active during the Tertiary (Civetta *et al.*, 1978; Peccerillo, 1985; Conticelli and Peccerillo, 1992). In such a scenario, it is important to understand how the intensive variables (P, T, fO_2) control the chemistry of phases such as Ti-andradite.

The thermal stability of Ti-andradite was investigated at atmospheric pressure by Huckenholz (1969). In that study, the maximum solubility of Ti in andradite was reported to be approximately 1.5 Ti atoms per formula unit in the range 1000-1300°C. At higher Ti contents, Ti-saturated andradite coexists with perovskite ($CaTiO_3$) and hematite (Fe_2O_3).

Since no data exist on the solubility of Ti in andradite at high pressures and temperatures, some preliminary data in upper mantle conditions are reported in this paper. They give some insights into the potential of garnet as a Ti reservoir in P-T conditions where magmas may be generated.

The structural position of Ti within andradite and its valence state are still subject of debate (e.g., Locock *et al.*, 1995; Malitesta *et al.*, 1995; Ambruster *et al.*, 1998): this issue will not be addressed here, although the experimental results might contribute to better understanding of the substitution mechanisms occurring in andradite. Moreover, although several authors (e.g., Manning and Harris, 1970; Huckenholz *et al.*, 1976; Huggins *et al.*, 1976; Kühberger *et al.*, 1989) report the presence of Ti^{3+} in Fe-rich garnet at relatively high fO_2 , we do not think it useful to discuss here the possible presence of Ti^{3+} in our synthetic garnets. Not only is there no need to invoke the presence of Ti^{3+} in recasting electron microprobe analyses, but the synthesis conditions were such as to exclude the

reduction of significant amounts of Ti^{4+} . Russell *et al.* (1999) recently proposed that the mechanisms of Ti entry into andradites allow a distinction between igneous and hydrothermal garnets and evaluation of the fO_2 and a_{SiO_2} conditions attending their formation.

EXPERIMENTAL DESIGN AND PROCEDURES

Starting material

In this work, two different starting materials with bulk compositions of Ti-saturated ($Ca_3Fe_2Ti_{1.5}Si_{1.5}O_{12}$) and Ti-undersaturated ($Ca_3Fe_2Ti_{0.75}Si_{2.25}O_{12}$) andradite with respect to 1 atm (Huckenholz, 1969) were chosen. They were synthesised in the following way. First, gels were prepared partially according to the procedure of Ito and Frondel (1967), the main difference consisting in the silica source; in our procedure, silica-free gels were prepared and mixed in appropriate amounts together with pure natural quartz (>99.9 wt% SiO_2). The mixtures were kept in a Pt crucible at 1100°C in air for about 30 days, with periodical regrinding and powder X-ray diffraction (XRD) checks. Hematite XRD peaks were initially the most intense ones, but their intensity diminished with the number of heating cycles. Syntheses were considered complete when hematite could no longer be detected by XRD. The products were mounted in epoxy resin and analysed by electron microprobe. Both materials consist mainly of Ti-andradite with minor amounts of pseudobrookite (Fe_2TiO_5) solid solution (Table 1). The Ti-undersaturated starting material also contained traces of rutile (TiO_2) and titanite ($CaTiSiO_5$), whereas minor glass ($SiO_2=45-50$ wt%, $TiO_2=10-12$ wt%, $FeO^*=15-16$ wt%, $CaO=3-5$ wt%) and traces of perovskite were present in the Ti-saturated starting material (Table 1). The grain size of phases were less than 30 μm . Unfortunately, electron microprobe analyses revealed that the starting materials had suffered some contamination by Na_2O and Al_2O_3 ; thus, garnets from Ti-undersaturated and Ti-saturated starting

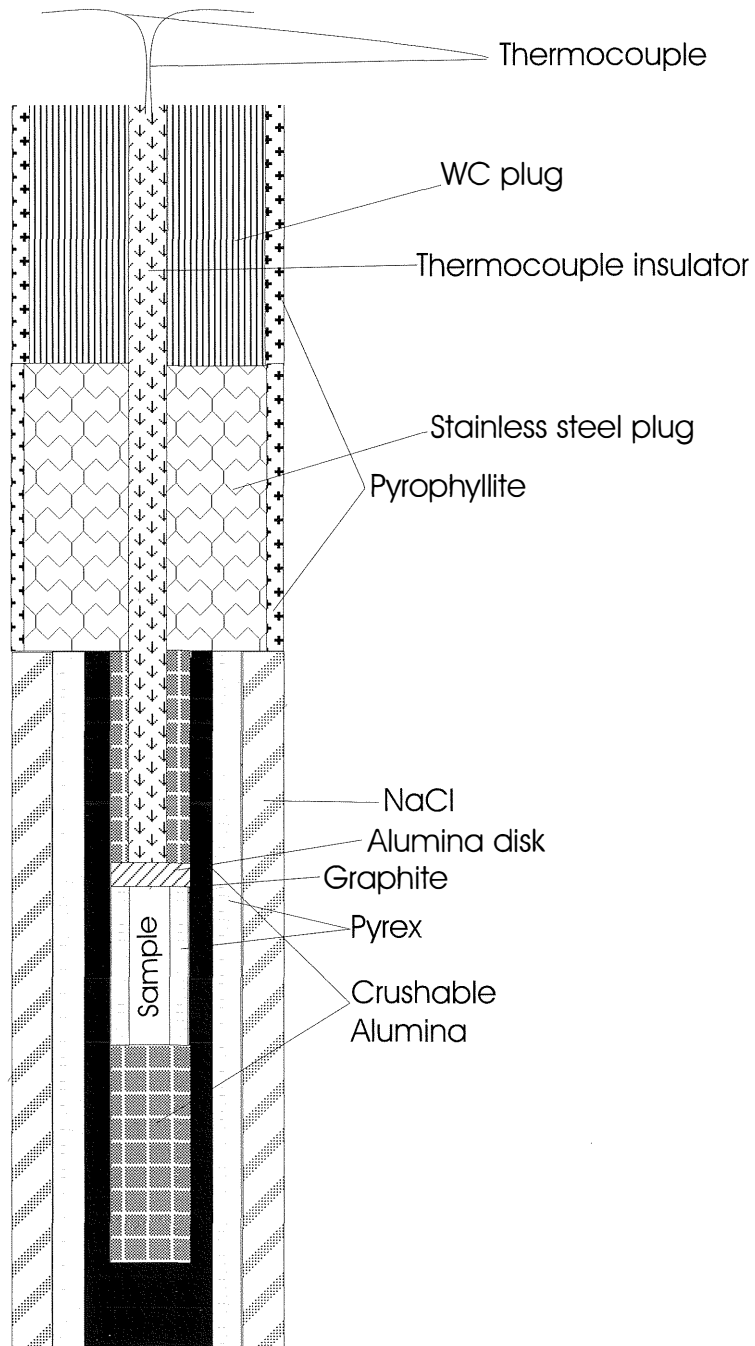


Fig. 1 – Sketch of assembly used for piston cylinder experiments. Width = 12.7 mm.

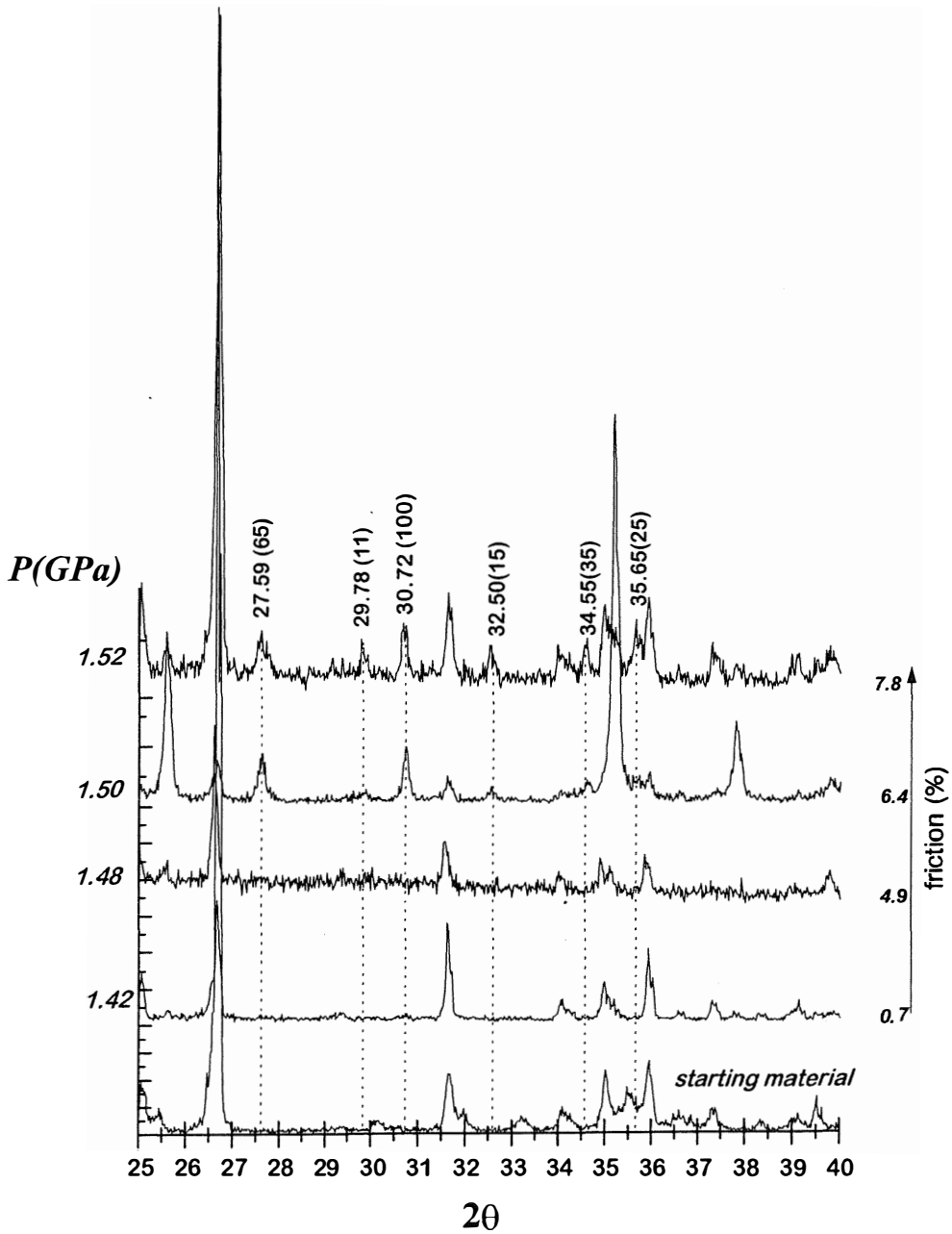


Fig. 2 – XRD spectra of products of calibration experiments performed at $T=1000^{\circ}\text{C}$. Dashed lines: ferrosilite peaks; top: positions and relative intensities (in brackets).

TABLE 1
Ideal chemical compositions and structural formulas of starting materials.

Bulk composition	Ideal formula	Products
Ti- undersaturated	$\text{Ca}_3\text{Fe}_2\text{Ti}_{0.75}\text{Si}_{2.25}\text{O}_{12}$	Ti-andradite, pseudobrookite, rutile, titanite
Ti- saturated	$\text{Ca}_3\text{Fe}_2\text{Ti}_{1.50}\text{Si}_{1.50}\text{O}_{12}$	Ti-andradite, pseudobrookite, perovskite, glass

materials contained up to 0.4 wt% (Na_2O) and 0.2 wt% (Al_2O_3) and up to 1.3 wt% (Na_2O) and 0.7 wt% (Al_2O_3) respectively.

Experimental procedures

Experiments were performed in a 0.5" piston cylinder at the Department of Earth Sciences, University of Florence. The instrument was modified with respect to the original design of Boyd and England (1960), being equipped with double-acting hydraulic cylinders of 100 and 75 tonnes capacity; the lower cylinder (75 tonnes) loads the high-pressure piston and the upper one provides extra force to end-load the pressure chamber.

Starting materials were loaded inside Pt capsules (5 mm long, O.D.=3.0 mm, I.D.=2.8 mm) and their ends were arc-welded shut. The assembly consisted of a NaCl/pyrex pressure medium, a graphite heater, and crushable alumina spacers (fig. 1). Temperature was measured by a Pt₁₀₀-Pt₉₀Rh₁₀ (type S) thermocouple, separated from the capsule by a thin alumina disk in order to prevent capsule piercing. No correction for pressure effects was applied to the thermocouple emf. The stainless steel and tungsten carbide plugs above the NaCl cell transmitted axial pressure and protected the top face of the chamber from radial pressure. Both plugs were electrically insulated from the pressure chamber by pyrophyllite sleeves. Temperature could be controlled to within 5°C of the stated values.

Experiments were performed in the P-T range 1.5-2.0 GPa at 1200-1300°C, with durations ranging from 1h 45min to 31h. Oxygen fugacity was neither controlled nor measured. No loss of Fe to the Pt container

occurred due to the subsolidus and significantly oxidising conditions of the experiments.

Pressure calibration

Pressure was calibrated at 1000°C using the 2FeSiO₃ (ferrosilite) = Fe₂SiO₄ (fayalite) + SiO₂ (quartz) transition (1.41 GPa, Bohlen *et al.*, 1980). Calibration experiments were performed using a mixture of pure synthetic fayalite (kindly provided by P. Ulmer, ETH, Zurich), quartz and ferrosilite, the latter phase being present in very small amounts. The XRD spectra (collected on a PW 1830 Philips diffractometer, Cu anticathode, 40 kV, 20 mA, counting times = 0.5 sec per 0.02°/2θ) of the products of four calibration experiments are shown in fig. 2. Ferrosilite growth began within the range 1.48-1.50 GPa, indicating that a friction of 5-6% must be taken into account when calculating the real pressure on the capsules.

Pressure calibration and all experiments were performed using the «cold piston-in» technique: the load was increased up to the working pressure at T=500°C. The temperature was then raised to the desired value. Quenching, obtained by interrupting the electric current through the graphite furnace, resulted in an initial quench rate of about 200-250°C/sec.

Analytical techniques

X-ray microanalyses of the experimental products were obtained by wavelength-dispersive spectrometry using a JEOL JXA-8600 electron microprobe, accelerating voltage 15 kV, beam current (monitored on a Faraday

TABLE 2
P-T-t conditions of experiments and experimental products.

Starting material	P (GPa)	T (°C)	t (h,m)	Products
Ti- undersaturated	2.0	1300	6 ^h	Ti-andradite, titanite
Ti- undersaturated	2.0	1200	31 ^h	Ti-andradite, titanite, hematite
Ti- saturated	2.0	1300	1 ^h 45 ^m	Ti-andradite, hematite
Ti- saturated	2.0	1200	8 ^h	Ti-andradite, perovskite, titanite, ilmenite, glass
Ti- saturated	2.0	1200	31 ^h	Ti-andradite, titanite, hematite
Ti- saturated	1.5	1300	6 ^h	Ti-andradite, hematite

cup) 10 nA, counting times on peak and background 20-40 seconds. The focused beam was about 1 μm across. Standards were: albite (SiK α and NaK α , TAP crystal), ilmenite (FeK α , LiF crystal; TiK α PET crystal) diopside (CaK α , PET crystal) and plagioclase (AlK α , TAP crystal). Data were corrected for the matrix effect using Bence and Albee's (1968) method, and errors (standard deviation <3%) were estimated according to Vaggelli *et al.* (1999).

RESULTS

Experimental run conditions of high-P experiments are shown in Table 2, together with the obtained products. Ti-andradites had extremely variable TiO₂ contents (9 - 25 wt%), depending on starting materials and P-T conditions of the run and were stable over the whole P-T range applied. Some representative analyses of Ti-andradites are shown in Table 3. Coexisting phases present in small amounts were titanite (CaTiSiO₅), hematite-ilmenite solid solution (Fe₂O₃ - FeTiO₃) and perovskite (CaTiO₃) (Table 4). The latter phase was only present in the 8^h run at 2 GPa and 1200°C and is probably metastable, because it was not found in the long-duration (31^h) run performed in the same P-T conditions. Thus, at 1200°C, titanite and hematite are the only stable phases coexisting with garnet, irrespective of the bulk composition of the starting materials.

DISCUSSION

Analyses of the two starting materials show that, at atmospheric pressure, Ti solubility in garnets (Table 3) is greater than that reported by Huckenholz (1969), in which the maximum degree of solid solution of Ca₃Fe₂Ti₃O₁₂ in garnet was reported to be 51.7 mol.% at T=1137°C. This is supported by the fact that some crystals have TiO₂ contents greater than expected (up to 28.8 wt%). Natural Fe,Ti-rich garnets with similar TiO₂ contents were reported by Grapes *et al.* (1979; TiO₂ = 27.4 wt%) and Mitchell and Meyer (1989, TiO₂ = 25.5 wt%).

The Ti contents of garnet originally synthesised from Ti undersaturated gel did not increase significantly at high P, whereas those found in garnet from Ti saturated starting materials decreased (Table 3, fig. 3). This indicates that maximum Ti contents in garnet decrease at high P with respect to 1 atm, although a «reservoir» from which additional Ti may be derived is available (Ti andradites coexist with Ti-bearing phases, Table 2). The large spread of TiO₂ values in some runs (fig. 3), particularly those performed at 2 GPa and 1300°C on a Ti- saturated andradite, indicate that equilibrium was not completely achieved. However, although reversal experiments aimed at evaluating the attainment of equilibrium were not performed, these data strongly indicate that, in the P-T range investigated, maximum Ti solubility in andradite is lower than that at 1 atm. Moreover, Ti solubility does

TABLE 3

Representative electron microprobe analyses of synthetic Ti-andradite. Fe²⁺ and Fe³⁺ calculated assuming stoichiometry and charge balance.

Start. Mat.	Ti-sat.	Ti-sat.	Ti-undersat.	Ti-sat.	Ti-sat.	Ti-sat.	Ti-sat.	Ti-sat.	Ti-sat.	Ti-sat.	Ti-sat.	Ti-undersat.	Ti-undersat.	Ti-undersat.	Ti-undersat.
P(GPa)/ T(°C)	-	-	-	2/1300	2/1300	2/1200	2/1200	2/1200	2/1200	1.5/ 1300	1.5/ 1300	2/1300	2/1300	2/1200	2/1200
t(h,m)	-	-	-	1.45	1.45	8	31	31	31	6	6	6	6	31	31
SiO ₂	17.9	18.9	29.6	22.9	23.1	25.5	25.2	25.0	22.1	23.9	22.0	26.2	26.5	28.1	27.3
TiO ₂	24.6	23.4	8.5	18.6	17.9	17.3	18.5	18.2	21.3	17.1	20.6	14.3	13.3	10.8	11.6
Al ₂ O ₃	0.66	0.51	0.11	1.45	1.44	1.37	1.73	1.58	1.16	1.20	1.30	0.21	0.22	0.27	0.17
FeO*	23.5	24.3	26.2	23.5	23.4	22.7	21.6	22.2	22.6	24.4	22.6	27.0	27.4	26.9	27.1
CaO	29.5	29.2	31.5	29.8	29.5	29.5	28.4	28.9	29.0	29.2	29.8	30.2	30.3	30.9	31.1
Na ₂ O	1.14	1.27	0.42	1.48	1.49	1.14	1.91	1.79	1.55	1.11	1.16	0.03	0.11	0.17	0.20
Sum	97.38	97.48	96.38	97.67	96.94	97.54	97.34	97.70	97.63	96.90	97.38	97.83	97.74	97.11	97.46
<i>Cations per 12 O:</i>															
Si	1.578	1.657	2.554	1.969	2.002	2.193	2.159	2.139	1.913	2.079	1.909	2.273	2.293	2.427	2.361
Al	0.069	0.053	0.011	0.147	0.147	0.139	0.175	0.159	0.118	0.123	0.133	0.021	0.022	0.028	0.017
Ti	1.634	1.542	0.553	1.201	1.166	1.119	1.195	1.170	1.384	1.115	1.348	0.931	0.865	0.702	0.752
Fe ³⁺	1.702	1.764	1.846	1.761	1.768	1.428	1.435	1.521	1.548	1.676	1.549	1.576	1.679	1.744	1.789
Fe ²⁺	0.034	0.023	0.051	0.000	0.000	0.210	0.112	0.069	0.089	0.102	0.092	0.387	0.305	0.207	0.170
Ca	2.788	2.744	2.915	2.747	2.738	2.721	2.607	2.646	2.688	2.718	2.774	2.807	2.816	2.864	2.876
Na	0.195	0.216	0.070	0.247	0.250	0.190	0.317	0.297	0.260	0.187	0.195	0.005	0.018	0.029	0.033
Sum	8.000	8.000	8.000	8.071	8.070	8.000	8.000	8.000	8.000	8.000	8.000	8.000	8.000	8.000	8.000
FeOc	0.46	0.31	0.70	0.00	0.00	2.92	1.56	0.97	1.23	1.40	1.27	5.32	4.21	2.86	2.35
Fe ₂ O ₃ c	25.62	26.67	28.38	26.09	26.05	22.03	22.24	23.63	23.74	25.60	23.65	24.09	25.71	26.75	27.50
Sumc	99.95	100.15	99.22	100.28	99.55	99.75	99.57	100.07	100.01	99.46	99.75	100.24	100.32	99.79	100.21
FeOc=FeO calculated, Fe ₂ O ₃ c=Fe ₂ O ₃ calculated, Sumc=Sum analysis considering FeOc and Fe ₂ O ₃ c.															

TABLE 4

Representative electron microprobe analyses of pseudobrookite (Psbr), hematite (Hem), ilmenite (Ilm), titanite (Tit) and perovskite (Pv). Fe²⁺ and Fe³⁺ calculated assuming stoichiometry and charge balance. X'Ilm calculated according to Stormer (1983).

Phase	Psbr		Hem	Hem	Hem	Hem	Hem	Hem	Hem	Hem	Hem
Start.Mat.	Ti-sat.		Ti-sat.	Ti-sat.	Ti-sat.	Ti-sat.	Ti-sat.	Ti-sat.	Ti-sat.	Ti-undersat.	Ti-undersat.
P/T	-		2/1300	2/1200	2/1200	2/1200	1.5/1300	1.5/1300	1.5/1300	2/1200	2/1200
t(h,m)	-		1.45	31	31	31	6	6	6	31	31
SiO ₂	0.05	SiO ₂	0.13	bdl	0.15	0.04	bdl	bdl	0.06	0.04	0.03
TiO ₂	33.3	TiO ₂	15.2	17.8	18.2	17.3	16.3	16.3	17.9	21.5	21.3
Al ₂ O ₃	0.42	Al ₂ O ₃	0.71	0.62	0.66	0.56	0.55	0.56	0.51	0.38	0.15
FeO*	58.0	FeO*	75.2	74.0	72.7	73.6	74.8	75.4	73.8	70.9	70.9
CaO	1.13	CaO	1.26	0.79	1.44	0.89	0.87	0.68	1.10	1.01	1.05
Na ₂ O	0.11	Na ₂ O	bdl	0.27	0.19	0.34	0.50	0.23	0.23	bdl	0.26
Sum	92.92	Sum	92.52	93.46	93.30	92.71	92.97	93.14	93.67	93.87	93.72
<i>Cat. per 5 O:</i>		<i>Cat. per 3 O:</i>									
Si	0.002	Si	0.003	0.000	0.004	0.001	0.000	0.000	0.002	0.001	0.001
Ti	1.001	Ti	0.299	0.349	0.355	0.342	0.321	0.320	0.350	0.420	0.419
Al	0.020	Al	0.022	0.019	0.020	0.017	0.017	0.017	0.016	0.012	0.005
Fe ³⁺	1.941	Ca	0.035	0.022	0.040	0.025	0.024	0.019	0.031	0.028	0.029
Ca	0.048	Fe ^{3+c}	1.374	1.283	1.262	1.297	1.341	1.343	1.281	1.145	1.156
Na	0.009	Fe ^{2+c}	0.267	0.327	0.319	0.318	0.297	0.301	0.321	0.393	0.390
Sum	3.021	Sum	2.000	2.000	2.000	2.000	2.000	2.000	2.000	2.000	2.000
FeOc	0.00	FeOc	12.24	15.01	14.66	14.47	13.54	13.80	14.79	18.12	17.88
Fe ₂ O _{3c}	64.41	Fe ₂ O _{3c}	69.96	65.51	64.52	65.68	68.02	68.42	65.61	58.65	58.91
		X'Ilm	0.29	0.34	0.35	0.34	0.32	0.32	0.34	0.42	0.41
Sumc	99.37	Sumc	99.53	100.02	99.76	99.29	99.78	99.99	100.24	99.75	99.62

TABLE 4: *continued*

Phase	Ilm	Ilm	Tit	Tit	Tit		Pv	Pv	
Start.Mat.	Ti-sat.	Ti-sat.	Ti-sat.	Ti-undersat.	Ti-undersat.		Ti-sat.	Ti-sat.	
P/T	2/1200	2/1200	2/1200	2/1200	2/1200		2/1200	2/1200	
t(h,m)	8	8	8	31	31		8	8	
SiO ₂	bdl	0.03	SiO ₂	30.3	30.2	30.4	SiO ₂	0.91	0.40
TiO ₂	34.1	34.1	TiO ₂	38.7	38.2	37.5	TiO ₂	55.6	56.3
Al ₂ O ₃	0.83	0.80	Al ₂ O ₃	0.63	0.05	0.07	Al ₂ O ₃	0.14	0.14
FeO*	59.1	60.1	FeO*	1.26	2.18	3.23	FeO*	1.97	1.41
CaO	1.38	1.01	CaO	28.4	28.5	28.2	CaO	40.0	40.4
Na ₂ O	0.38	0.52	Na ₂ O	0.11	0.14	0.10	Na ₂ O	0.62	0.50
Sum	95.80	96.50	Sum	99.35	99.30	99.44	Sum	99.27	99.11
<i>Cat. per 3 O:</i>			<i>Cat. per 20 O:</i>			<i>Cat. per 3 O:</i>			
Si	0.000	0.001	Si	3.996	4.015	4.044	Si	0.021	0.009
Ti	0.662	0.658					Al	0.004	0.004
Al	0.025	0.024	Al	0.098	0.008	0.011	Ti	0.945	0.959
Ca	0.038	0.028	Ti	3.846	3.820	3.751	Fe ^{3+c}	0.093	0.083
Fe ^{3+c}	0.650	0.658	Fe ²⁺	0.139	0.242	0.360	Fe ^{2+c}	0.000	0.000
Fe ^{2+c}	0.624	0.631	Sum Y	4.084	4.071	4.122	Ca	0.967	0.980
Sum	2.000	2.000					Na	0.027	0.022
			Ca	4.014	4.057	4.021	Sum	2.056	2.056
FeOc	28.94	29.40	Na	0.028	0.036	0.026			
Fe ₂ O _{3c}	33.50	34.07	Sum X	4.042	4.094	4.047	FeOc	0.00	0.00
X' Ilm	0.66	0.66					Fe ₂ O _{3c}	2.19	1.57
Sumc	99.16	99.91	Sum cat.	12.12	12.18	12.21	Sumc	99.49	99.27

FeOc=FeO calculated, Fe₂O_{3c}=Fe₂O₃ calculated, Sumc=Sum analysis considering FeOc and Fe₂O_{3c}. bdl=below detection limit.

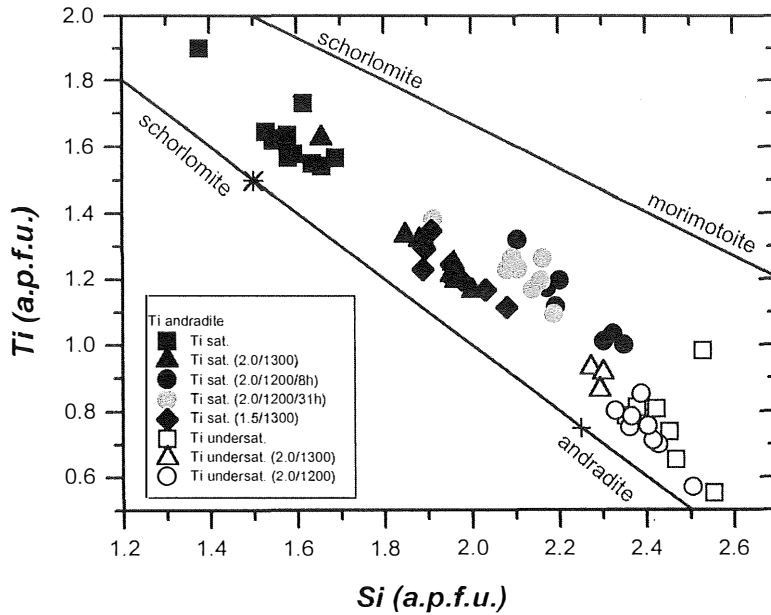


Fig. 3 – Si versus Ti of Ti-andradites (a.p.f.u.: atoms per formula unit) synthesised from gels and resulting from high-P experiments. Bulk compositions of Ti- saturated (*) and Ti- undersaturated (+) starting materials are also shown.

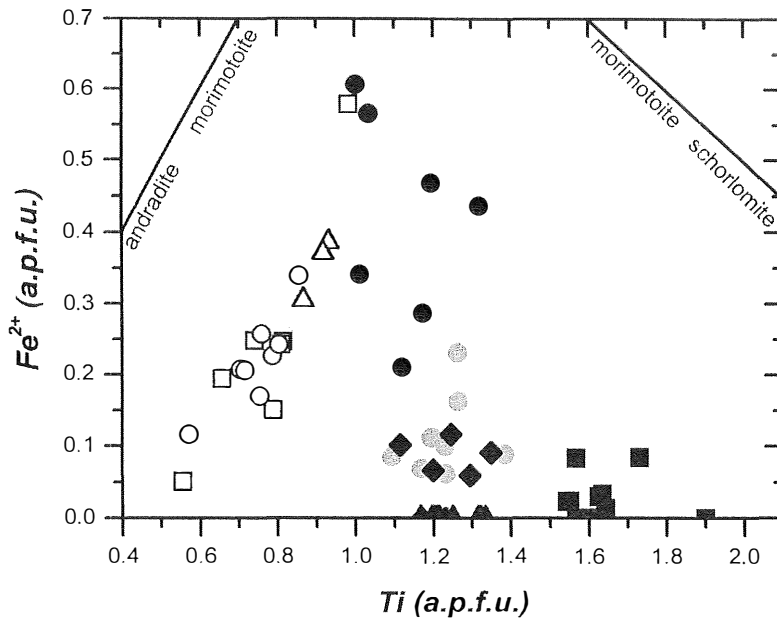


Fig. 4 – Ti versus Fe^{2+} of Ti-andradites synthesised from gels and resulting from high-P experiments (symbols as in fig. 3).

not vary significantly with pressure from 1.5 to 2.0 GPa (at 1300°C, fig. 3); moreover, at these pressures, Ti solubility in garnet does not seem to be temperature-dependent, in a different way as occurs at 1 atm (Huckenholz, 1969). Nevertheless, it must be considered that oxygen fugacity was not controlled during the experiments; as a matter of fact, Ti solubility in garnet almost certainly depends also on this variable.

Incorporation of Ti in the garnet structure may be attributed to substitution along the exchange vector $Ti^{4+}Si^{4+}_{-1}$ (fig. 3). This is called *schorlomitic* substitution (e.g., Ambruster *et al.*, 1998), in which Ti^{4+} preferentially occupies the octahedral site and Fe^{3+} mainly occupies the tetrahedral site. The other main substitution mechanism revealed in natural Ti-andradites is the so-called *morimotoitic* substitution (e.g., Henmi *et al.*, 1995), in which substitution in the octahedral site occurs as the exchange vector $Fe^{2+}Ti^{4+}Fe^{3+}_{-2}$. This substitution is represented in a Ti vs Fe^{2+} graph (fig. 4), in which some correlation between these variables should be expected. It appears that this substitution may be important only in Ti-undersaturated andradites, and it is certainly absent in Ti-saturated ones, if it is assumed that Ti^{3+} plays no major role or none at all. Considering natural andradites, both *schorlomitic* and *morimotoitic* substitutions are usually coupled to a certain extent to hydrogarnet substitution $(O_4H_4)(SiO_4)_{-1}$ (e.g., Ambruster *et al.*, 1998). This is obviously not the case for the garnets synthesised in the present work, because syntheses were performed in dry conditions.

CONCLUSIONS

These experimental results indicate that Ti solubility in synthetic andradites decreases from 1 atm to 1.5-2.0 GPa (at 1200-1300°C), since Ti decreases from 1.5-2.0 a.p.f.u. (at 1 atm.) down to 1.0-1.4 a.p.f.u. at high P. Moreover, in this P range, Ti solubility does not seem to be related with temperature.

Schorlomitic substitution is the main mechanism responsible for Ti entry into the garnet structure, whereas *morimotoitic* substitution may have importance only in Ti-undersaturated andradites. Moreover, at atmospheric pressure, Ti solubility in andradites seems to be greater than reported by Huckenholz (1969).

ACKNOWLEDGMENTS

The manuscript benefited by revision from U. Söffler and Y. Thibault; their comments and suggestion notably improved the paper. The authors wish to thank S. Conticelli for supporting and stimulating this research and F. Olmi for assistance during electron microprobe analyses. Financial support was provided by Italian M.U.R.S.T. through the «Cofin '98» project on «Terrestrial materials and synthetic analogues at high pressure and high temperature: physical, chemical and rheologic properties» to S. Tommasini, and C.N.R. contribution # 9800584CT11 to S. Conticelli.

REFERENCES

- AMBRUSTER T., BIRRER J., LIBOWITZKY E. and BERAN A. (1998) — *Crystal chemistry of Ti-bearing andradites*. *Eur. J. Mineral.*, **10**, 907-921.
- BENCE A.E. and ALBEE A.L. (1968) — *Empirical correction factors for the electron microanalysis of silicates and oxides*. *J. Geol.*, **76**, 382-402.
- BOHLEN S.R.B., ESSENE E.J. and BOETTCHER A.L. (1980) — *Reinvestigation and application of olivine-quartz-orthopyroxene barometry*. *Earth Planet. Sci. Lett.*, **47**, 1-10.
- BOYD F.R. and ENGLAND J.L. (1960) — *Apparatus for phase-equilibrium measurements at pressures up to 50 kilobars and temperatures up to 1750°C*. *J. Geoph. Res.*, **65**, 741-748.
- CAGGIANELLI A., DE FINO M., LA VOLPE L. and PICCARRETA G. (1990) — *Mineral chemistry of Monte Vulture volcanics: petrological implications*. *Mineral. Petrol.*, **41**, 215-227.
- CIVETTA L., ORSI G., SCANDONE P. and PECE R. (1978) — *Eastwards migration of the Tuscan anatectic magmatism due to anticlockwise rotation of the Appennines*. *Nature*, **276**, 604-606.
- CONTICELLI S. and PECCERILLO A., (1992) — *Petrology and geochemistry of potassic and ultrapotassic volcanism in central Italy*;

- petrogenesis and inferences on the evolution of the mantle.* *Lithos*, **28**, 221-240.
- DE FINO M., LA VOLPE L., PECCERILLO A., PICCARRETA G. and POLI G. (1986) — *Petrogenesis of Monte Vulture volcano (Italy): inferences from mineral chemistry, major and trace element data.* *Contrib. Mineral. Petrol.*, **92**, 135-145.
- GRAPES R., YAGI K. and OKUMURA K. (1979) — *Aenigmatite, sodic pyroxene, arfvedsonite and associated minerals in syenites from Morotu, Sakhalin.* *Contrib. Mineral. Petrol.*, **69**, 97-103.
- HENMI CH., KUSACHI I. and HENMI K. (1995) — *Morimotoite, $Ca_3Ti Fe^{2+}Si_3O_{12}$, a new titanian garnet from Fuku, Okayama Prefecture, Japan.* *Mineral. Mag.*, **59**, 115-120.
- HOWIE R.A. and WOOLLEY, A. R. (1968) — *The role of titanium and the effect of TiO_2 on the cell-size, refractive index, and specific gravity in the andradite - melanite - schorlomite series.* *Mineral. Mag.*, **36**, 775-790.
- HUCKENHOLZ H.G. (1969) — *Synthesis and stability of Ti-andradite.* *Am. J. Sci.*, **267A**, 209-232.
- HUCKENHOLZ H.G. and YODER H.S. (1971) — *Andradite stability relations in the $CaSiO_3$ - Fe_2O_3 join up to 30 Kb.* *N. Jahrb. Mineral. Abh.*, **114**, 246-280.
- HUCKENHOLZ H.G., HOELZL E., HUGGINS F.E. and VIRGO D. (1976) — *A reconnaissance study of the Ti-garnet stability field at defined oxygen fugacities.* *Carn. Inst. of Washington Year Book*, **75**, 711-720.
- HUGGINS F.E., VIRGO D. and HUCKENHOLZ H. (1976) — *The crystal chemistry of melanites and schorlomites.* *Carn. Inst. of Washington Year Book*, **75**, 705-711.
- ITO J. and FRONDEL C. (1967) — *Synthetic zirconium and titanium garnets.* *Am. Mineral.*, **52**, 773-781.
- KÜHBERGER A., FEHR T., HUCKENHOLZ H.G., and AMTHAUER G. (1989) — *Crystal chemistry of a natural schorlomite and Ti-andradites synthesised at different oxygen fugacity.* *Phys. Chem. Mineral.*, **16**, 734-740.
- LANG J.R., STANLEY C.R., THOMPSON J.F.H., and DUNNE K.P.E. (1995) — *Na-K-Ca magmatic-hydrothermal alteration in alkalic porphyry Cu-Au deposits, British Columbia.* In *Magma, fluids and ore deposits.* J.F.G. Thompson, ed. *Mineral. Assoc. Can. Short Course Series*, **23**, 339-365.
- LOCOCK A., LUTH R.W., CAVELL R.G., SMITH D.G.W. and DUKE M.J.M. (1995) — *Spectroscopy of the cation distribution in the schorlomite species of garnet.* *Amer. Mineral.*, **80**, 27-38.
- MALITESTA C., LOSITO I., SCORDARI F. and SCHINGARO E. (1995) — *XPS investigation of titanium in melanites from Monte Vulture (Italy).* *Eur. J. Mineral.*, **7**, 847-858.
- MANNING P.G. and HARRIS D.C. (1970) — *Optical-absorption and electron-microprobe studies of some high-Ti andradites.* *Can. Mineral.*, **10**, 260-271.
- MELLUSO L., MORRA V. and DI GIROLAMO P. (1996) — *The Mount Vulture Volcanic Complex (Italy): evidence for distinct parental magmas and for residual melts with melilite.* *Mineral. Petrol.*, **56**, 225-250.
- MITCHELL R.H. and MEYER H.O.A. (1989) — *Mineralogy of micaceous kimberlites from the new Elands and Star Mines, Orange Free State, South Africa.* *Geological Society of Australia Spec. Publ.*, **14**, 83-96.
- PECCERILLO A. (1985) — *Roman comagmatic province (central Italy): evidence for subduction-related magma genesis.* *Geology*, **13**, 103-106.
- RUSSELL J.K., DIPPLE G.M., LANG J.R. and LUECK B. (1999) — *Major-element discrimination of titanian andradite from magmatic and hydrothermal environments: an example from the Canadian Cordillera.* *Eur. J. Mineral.*, **11**, 919-935.
- STORMER J.C. (1983) — *The effects of recalculation on estimates of temperature and oxygen fugacity from analyses of multicomponent iron-titanium oxides.* *Am. Mineral.*, **68**, 586-594.
- VAGGELLI G., OLMÍ F. and CONTICELLI S. (1999) — *Quantitative electron microprobe analysis of reference silicate mineral and glass samples.* *Acta Vulcanologica*, **11**, 297-303.